

Excited-State Absorption by Linear Response Time-Dependent Density Functional Theory

Xiaowei Sheng,* Hongjuan Zhu, Kai Yin, Jichao Chen, Jian Wang,* Chunrui Wang, Junfeng Shao, and Fei Chen

Cite This: *J. Phys. Chem. C* 2020, 124, 4693–4700

Read Online

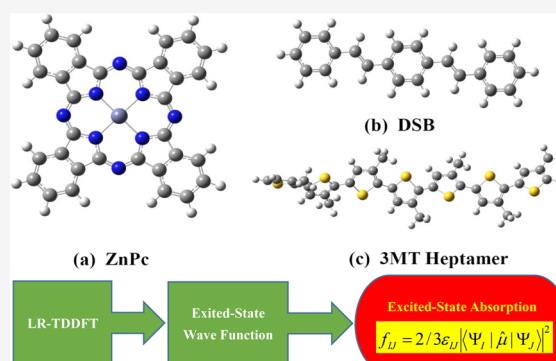
ACCESS |

Metrics & More

Article Recommendations

Supporting Information

ABSTRACT: Investigations of the ground and excited states absorption are very important for the development of advanced optical limiters. Linear response time-dependent density-functional theory (LR-TDDFT) has become popular for calculating absorption spectra of molecules in their ground state. However, calculation for the excited state turns out to be much more complicated. In the present paper, it is shown that the transition dipole moments between two excited states can be well-estimated based on auxiliary excited-state wavefunctions extracted from the LR-TDDFT calculation. For application, the absorption spectra in zinc phthalocyanine (ZnPc), distyrylbenzene (DSB), and 3-methylthiophenes heptamer (3MT heptamer) are investigated in detail along with different density functional models, and results are compared with experimental data and other theoretical methods. The computational cost of the present method is much cheaper than other theoretical methods, such as quadratic response TDDFT.



I. INTRODUCTION

With the rapid development of intense light sources, more and more researchers realized that designing materials for protecting the light-sensitive materials is urgent.¹ Developing optical power limiting (optical limiting) materials is one of the most possible solutions for this issue.^{2–7} These materials show a strong attenuation of light transmission at high input intensities but have a very high transmittance for the light at low input intensities.^{5,6} It is well-known that reversed saturation absorption (RSA) is one of the most important non-linear optical properties for the materials showing an optical-limiting character. The necessary condition for the materials showing a reversed saturation absorption property is that the excited states have higher absorption than the ground state.⁸ Therefore, the knowledge of absorption spectra of the molecules in both the ground and excited states are important for the study of optical-limiting materials.^{9–13}

Linear response time-dependent density-functional theory (LR-TDDFT) is one of the most popular methods to study absorption spectra in molecules and solids. Up to now, most studies focused on ground-state absorption (GSA), and results in most cases are in good agreement with experimental data.^{14–20} For excited-state absorption (ESA), instead of a linear response, one in theory need quadratic response TDDFT (QR-TDDFT)^{8,21–28} The computational cost of QR-TDDFT is much expensive, scaling as N^6 . Other approximate but less expensive methods to calculate ESA are also available.^{8,25,27,28}

Mikhailov et al. proposed a modified linear response Tamm–Dancoff equation to calculate the transition moments between excited states (a posteriori TDA, ATDA), and their results compare well to those from QR-TDDFT.^{25,29,30} Fischer et al.⁸ developed a real-time TDDFT (RT-TDDFT) method to extract ESA in which an excited initial reference was propagated in real time. It was demonstrated that this method can efficiently predict the optical limiting character of a molecular complex.⁸ Mosquera et al. introduced a second linear-response method (SLR) to obtain ESA for diplatinum(II) complex and many conjugated polymers.^{27,28} The cost of SLR is only twice that of LR-TDDFT.

In this paper, we present an efficient method to calculate ESA in which approximate excited-state wavefunctions are constructed from the LR-TDDFT calculation. The method is illustrated in section II. We then apply it to the molecules of zinc phthalocyanine (ZnPc), distyrylbenzene (DSB), and 3-methylthiophenes heptamer (3MT heptamer), and various density functionals are chosen to compare the results, as presented in section III. Further discussion is in section IV, and section V is the conclusion.

Received: November 4, 2019

Revised: January 25, 2020

Published: February 4, 2020

II. METHODS

We assume that the state i is the target excited state, and the oscillator strength for the transition of $i \rightarrow j$ can be represented as

$$f_{ji} = 2/3\varepsilon_{ji}|\langle\Psi_i|\hat{\mu}|\Psi_j\rangle|^2 \quad (1)$$

where ψ_i and ψ_j are the excited-state wavefunctions, $\hat{\mu}$ is the dipole vector operator, and $\varepsilon_{ji} = E_j - E_i$ is the excitation energy. ε_{ji} and the wavefunction of excited-state ψ have to be known to calculate the oscillator strength f_{ij} . The excitation energy ε_{ji} can be obtained from the LR-TDDFT calculations. For the wavefunctions of excited-state ψ , the following approximation is used in the present paper.^{31–40}

$$\Psi_i = \sum_{m \rightarrow a} C_m^a \Phi_m^a + \sum_{m \leftarrow a} C_m^a \Phi_m^a \quad (2)$$

$$= \sum_m^{\text{occ}} \sum_a^{\text{vir}} C_m^a \Phi_m^a + \sum_m^{\text{occ}} \sum_a^{\text{vir}} C_m^a \Phi_m^a \quad (3)$$

where m and a run over all occupied and all unoccupied orbitals respectively. Φ_m^a represents the configuration, which is constructed by moving an electron from the occupied orbital m to the virtual orbital a . C_m^a is the contribution from excitation, while C_m^a is the contribution from de-excitation. The configuration coefficients C_m^a and C_m^a are related to the X and Y vectors of the following non-Hermitian eigenvalue equation of LR-TDDFT, respectively.^{36,35,40}

$$\begin{bmatrix} A & B \\ B^* & A^* \end{bmatrix} \begin{bmatrix} X \\ Y \end{bmatrix} = \omega \begin{bmatrix} 1 & 0 \\ 0 & -1 \end{bmatrix} \begin{bmatrix} X \\ Y \end{bmatrix} \quad (4)$$

The details of the matrices A and B can be found in ref 32. According to Casida, eq 3 is assigned as (up to a normalization factor)⁴⁰

$$\Psi_i = \sum_m^{\text{occ}} \sum_a^{\text{vir}} (X_{am}^i + Y_{am}^i) \Phi_m^a \quad (5)$$

With the above formulation, once the LR-TDDFT equations are solved, the wavefunctions for the excited states can be constructed, and then the oscillator strengths for transition between any two excited states are calculated using eq 1. The absorption spectrum is then collected from the oscillator strengths at a given excitation energy broadened with a Gaussian function (FWHM = 0.4 eV). To validate the present scheme, the absorption spectra of zinc phthalocyanine (ZnPc, C₃₂H₁₆N₈Zn), distyrylbenzene (DSB, C₂₂H₁₈), and 3-methylthiophenes heptamer (3MT heptamer, C₃₅H₃₀S₇) from the first singlet excited states are investigated and compared with experimental data and other theoretical calculations, if available. All the valence orbitals (C 2s²2p², H 1s¹, N 2s²2p³, Zn 3d¹⁰4s², S 3s²3p⁴) are included in the orbital space. To see the effect of different DFT functionals, we choose functional models with different percentages of exact-exchange (Hartree-Fock, HF) character (B3LYP, 20% HF; M06, 27% HF; BHandHLYP, 50% HF; CAM-B3LYP, SR19% HF, LR65% HF; ω B97XD, SR22.2% HF, LR100% HF).^{41–45} All the calculations are performed under the 6-31G(d,p) basis set, which have been documented in previous works.^{8,11,9,46} The basis set dependence also has been shown in Table S1. It is confirmed that 6-31G(d,p) is enough for the present investigations. A modified code based

on the GAMESS(US) package⁴⁷ has been developed for the calculation and analysis.

III. RESULTS

A. Excited-State Absorption Spectra. Figure 1 shows the geometries of ZnPc, DSB, and 3MT heptamer. It shows that

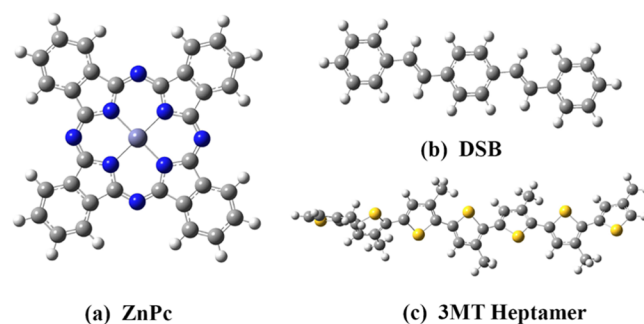


Figure 1. Geometries of ZnPc, DSB, and 3MT heptamer optimized at the BHandHLYP/6-31G(d,p) level in the ground state. White, grey, blue, and yellow spheres represent the hydrogen, carbon, nitrogen, and sulfur atoms, respectively. (a) ZnPc. (b) DSB. (c) 3MT heptamer.

three molecules have different structures. All the atoms in ZnPc or DSB are in the same plane. However, DSB has a chain structure, which is different from ZnPc. 3MT heptamer also has a chain structure but the atoms are nonplanar. Cartesian coordinates of these molecules in the ground state S_0 are listed in the Supporting Information (Table S2).

1. Excited-State Absorption Spectrum of ZnPc. ZnPc has attracted lots of attention because of its optical-limiting property. It has been well-studied both theoretically and experimentally.^{8,14} In their experiment, Savolainen et al.¹⁴ recorded the spectrally resolved pump–probe data of zinc phthalocyanine on time scales ranging from femtoseconds to nanoseconds. They observed two distinct bands peaking at 1.97 and 2.56 eV for the first singlet excited state. In order to simulate the absorption spectrum properly, transitions from the first singlet excited state to 50 singlet excited states above are taken into account. Since the measurements were conducted in the solvent DMSO, its effect is simulated with a polarizable continuum model (PCM). The calculated first singlet ESA spectra with various functionals employed are shown in Figure 2, with the peak positions in the spectra listed in Table 1.

Among the functionals investigated, BHandHLYP functional seems to be the best functional for this system. The peaks in Figure 2 are at 1.97, 2.53, and 3.80 eV, respectively. The first peak is in excellent agreement with the experimental data, while the transition energy is underestimated by 0.03 eV for the second peak. It is to be noted that our calculation shows a third peak around 3.80 eV; however, experimental data is still missing because Savolainen et al. measured the ESA spectrum only up to 2.76 eV.¹⁴

It is obvious that ESA spectrum depends on the functional employed in the TDDFT calculations. For the hybrid functionals of B3LYP and M06, which have less components of exact-exchange compared with BHandHLYP, the transition energies of the first peak are underestimated by 0.4 and 0.21 eV respectively. Table 1 and Figure 2a show that the predicted transition energies increase with the amount of exact-exchange included in the functional. For this system, functionals with ~50% exact-exchange may be a good choice for the transition

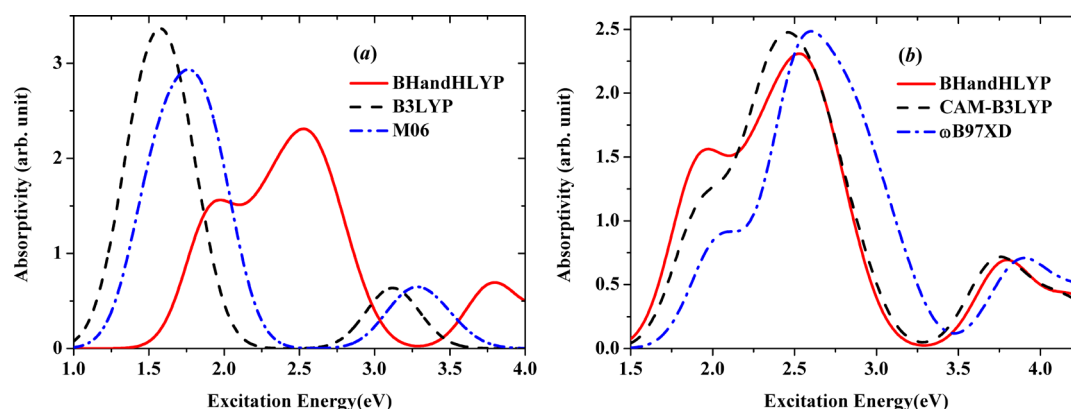


Figure 2. Simulated absorption spectrum for ZnPc from the first singlet excited state (S_1) with various functionals employed. The spectra are obtained using the calculated oscillator strengths and the excitation energies broadened with a Gaussian function (FWHM = 0.4 eV). The red solid line is the result of BHandHLYP, which is in excellent agreement with the experimental data. (a) Hybrid functionals are employed. (b) Long-range corrected functionals are employed.

Table 1. Positions of Prominent Features in the First Singlet Excited-State Absorption Spectrum of ZnPc^a

functional	1st peak	2nd peak	3rd peak
exp ^b	1.97	2.56	NA
RT-TDDFT ^c	2.24	2.84	NA
B3LYP ^d	1.57	3.12	NA
M06 ^d	1.76	3.28	NA
BHandHLYP ^d	1.97	2.53	3.80
CAM-B3LYP ^d	2.46	3.76	NA
ω B97XD ^d	2.60	3.90	NA

^aAll values are in electron volts (eV). ^bTaken from ref 14. ^cTaken from ref 8. ^dThe present results.

energies. Those results are also consistent with the previous observations.^{48,49} For the long-range corrected functionals CAM-B3LYP and ω B97XD shown in Figure 2b, the first peak is less prominent, while the second peak (2.56 eV) of the experimental result is well-predicted. It is also noticed that the transition energy predicted by ω B97XD is larger than that of CAM-B3LYP, which may be expected because the percentage of exact-exchange in ω B97XD is higher than that of CAM-B3LYP at both short and long ranges. In Table 1, the list of RT-TDDFT is from Fischer et al.,⁸ only two peaks are predicted based on RT-TDDFT calculations with CAM-B3LYP. The two peaks

overestimate the transition energies by 0.27 and 0.28 eV, respectively, compared with the experimental data.

2. *Excited-State Absorption Spectrum of DSB.* The ESA spectrum of DSB has been well-studied in the experiment.^{11,50} In their experiment (conducted in dioxane), Oliveira et al.¹¹ observed that the main band of the first singlet ESA centers at

Table 2. Position of Prominent Features in the First Singlet Excited-State Absorption Spectrum of DSB^a

functional	position
exp ^b	1.67
QR-TDDFT (CAM-B3LYP) ^b	1.51
B3LYP ^c	0.82
M06 ^c	1.01
BHandHLYP ^c	1.60
CAM-B3LYP ^c	1.66
ω B97XD ^c	1.89

^aAll values are in electron volts (eV). ^bTaken from ref 11. ^cThe present results.

1.67 eV. Our calculation results are shown in Figure 3 and Table 2. Likewise, the solvent effect is taken into account using the PCM model. Transition from the first singlet excited state to the

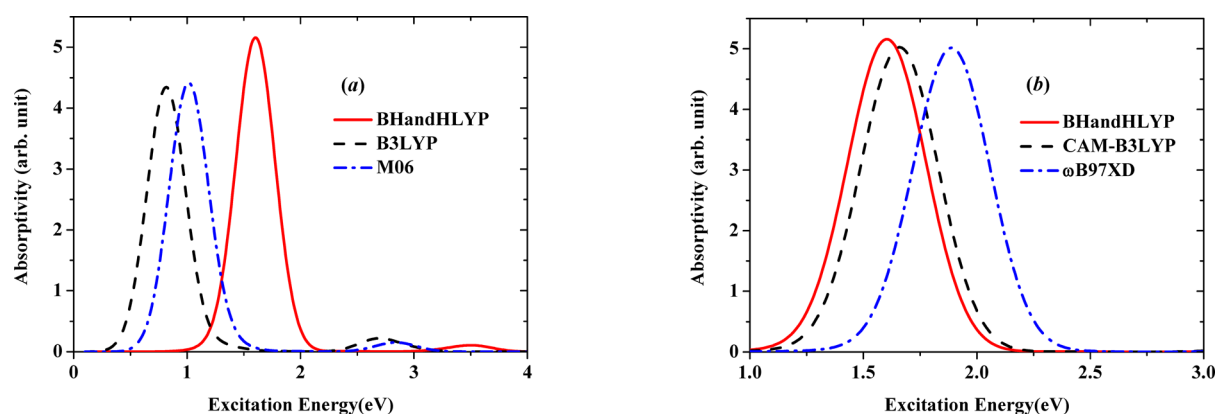


Figure 3. Simulated absorption spectrum for DSB from the first singlet excited state (S_1) with various functionals employed. The spectra are obtained using the calculated oscillator strengths and the excitation energies broadened with the Gaussian function (FWHM = 0.4 eV). (a) Hybrid functionals are employed. (b) Long-range corrected functionals are employed.

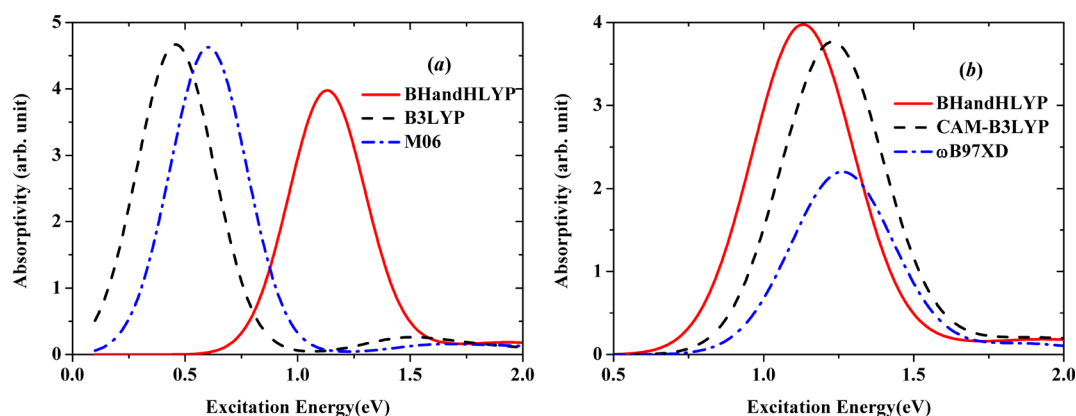


Figure 4. Simulated absorption spectrum for 3MT heptamer in the first singlet excited state (S_1) with various functionals employed. The spectra are obtained using the calculated oscillator strengths and the excitation energies broadened with the Gaussian function (FWHM = 0.4 eV). The red solid line is the result of BHandHLYP, which is in excellent agreement with the experimental measurement. (a) Hybrid functionals are employed. (b) Long-range corrected functionals are employed.

20 singlet excited states above are considered to obtain the absorption spectrum.

The peak position depends on the functional employed. For the hybrid functional BHandHLYP, the predicted main band centers at 1.60 eV, which underestimates the experimental result by only 0.07 eV. For the other two hybrid functionals, B3LYP and M06, both underestimate the transition energy. For the long-range corrected functional CAM-B3LYP, the predicted transition energy (1.66 eV) is in excellent agreement with the experimental result (1.67 eV), while that by ω B97XD is higher than CAM-B3LYP and overestimate the experimental result by 0.22 eV. Oliveira et al. also performed QR-TDDFT calculations for DSB.¹¹ The first band peak is underestimated by 0.16 eV.

3. Excited-State Absorption Spectrum of 3MT Heptamer. 3MT heptamer is interesting because its ESA is in excellent agreement with the most studied conjugated polymers (3-hexylthiophene, P3HT).⁹ The ESA spectrum of P3HT from the first singlet excited state was measured in THF (tetrahydrofuran) by Tapping and Kee.⁵¹ The measured position of the band peak is 1.17 eV. Roseli et al.⁹ showed that the solvent effect is minor, that is, inclusion of a solvent leads to similar results as in vacuum. Consequently, we calculated the singlet excited states ESA of 3MT heptamer in vacuum. Here, the first 20 singlet excited states of 3MT heptamer have been considered to simulate the spectrum. Figure 4 displays the absorption spectra curves, and Table 3 presents the peak position of the absorption spectra.

For the hybrid functional BHandHLYP, the predicted (1.13 eV) and experimental observed band peaks (1.17 eV) differ by

Table 3. Position of Prominent Features in the First Singlet Excited-State Absorption Spectrum of 3MT Heptamer^a

functional	position
exp ^b	1.17
QR-TDDFT (CAM-B3LYP) ^c	1.22
B3LYP ^d	0.46
M06 ^d	0.60
BHandHLYP ^d	1.13
CAM-B3LYP ^d	1.23
ω B97XD ^d	1.26

^aAll values are in electron volts (eV). ^bTaken from refs 51, 52. ^cTaken from ref 9. ^dThe present results.

only 0.04 eV, which is much better than the other two hybrid functionals B3LYP and M06. The second peak is very weak compared with the first one, almost unobservable in the scale of Figure 4. For the long-range corrected functionals CAM-B3LYP and ω B97XD, the predicted value based on the CAM-B3LYP functional (1.23 eV) is closer to the experimental result of P3HT compared with the functional ω B97XD (1.26 eV). The trends are similar to those in ZnPc and DSB in the above subsections. Roseli et al. reported QR-TDDFT calculations with the CAM-B3LYP functional.⁹ Their prediction peak at 1.22 eV is almost coincident with our value at 1.23 eV.

B. Effect of de-Excitation on the ESA. To get insight into the contribution of de-excitation configurations in eqs 2 and 3, we also performed the TDDFT calculation with the Tamm–Dancoff approximation (TDA/TDDFT).^{53,54} According to this approximation, the excited-state wavefunction ψ_i can be written as

$$\Psi_i = \sum_{m \rightarrow a} C_m^a \Phi_m^a = \sum_m \sum_a C_m^a \Phi_m^a = \sum_m \sum_a X_{am}^i \Phi_m^a \quad (6)$$

All of the de-excitation contribution represented by the “Y” vector is ignored. The wavefunction constructed in this way is the same as the configuration interaction with single excitation (CIS).⁵⁴ However, the Kohn–Sham orbitals are used here rather than the Hartree–Fock orbitals in CIS. In addition, the coefficients of the configurations are obtained in different ways.⁵² Our calculations for ZnPc, DSB, and 3MT heptamer show that the present scheme is much more accurate than CIS.

Figure 5 displays the spectra. It is clearly shown that the spectra derived by the TDA/TDDFT have a small red shift compare with the TDDFT results. The largest red shift is 0.21 eV, which is the second absorption peak of ZnPc. In the case of 3MT heptamer, the red shift is only 0.09 eV (see Figure S1 in the Supporting Information). Therefore, Tamm–Dancoff approximation is a very good approximation. This is also consistent with the previous observations.^{54,55} For comparison, the CIS calculations have also been calculated for ZnPc, DSB, and 3MT heptamer. For ZnPc, the peak at 1.97 eV is missed with the CIS method. The first peaks for DSB and 3MT heptamer based on the CIS method, at 2.95 and 2.28 eV, respectively, are quite away from the peaks of TDDFT and TDA/TDDFT. This is expected because CIS is not a good approximation to describe the excited states.

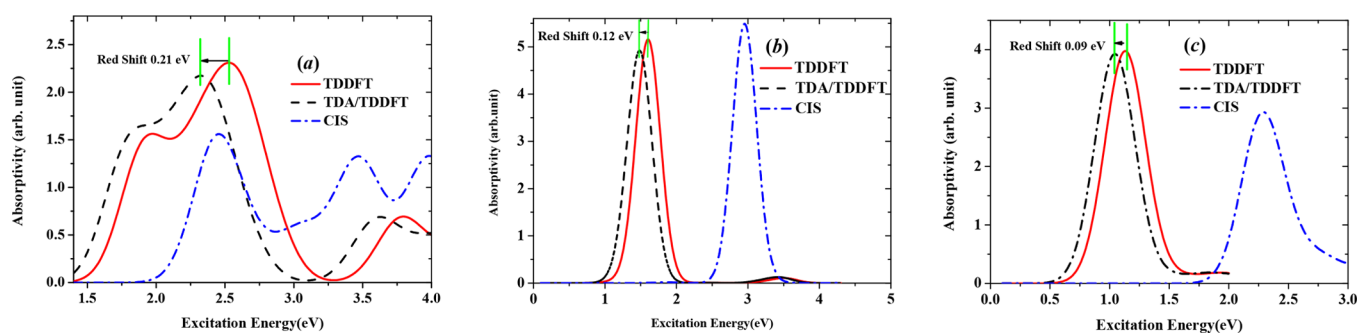


Figure 5. Simulated absorption spectra for ZnPc, DSB, and 3MT heptamer from the first singlet excited state (S_1) based on the TDDFT, TDA/TDDFT, and CIS theories. The hybrid functional of BHandHLYP was employed, and the spectra are obtained using the calculated oscillator strengths and the excitation energies broadened with the Gaussian function (FWHM = 0.4 eV). (a) ZnPc. (b) DSB. (c) 3MT heptamer.

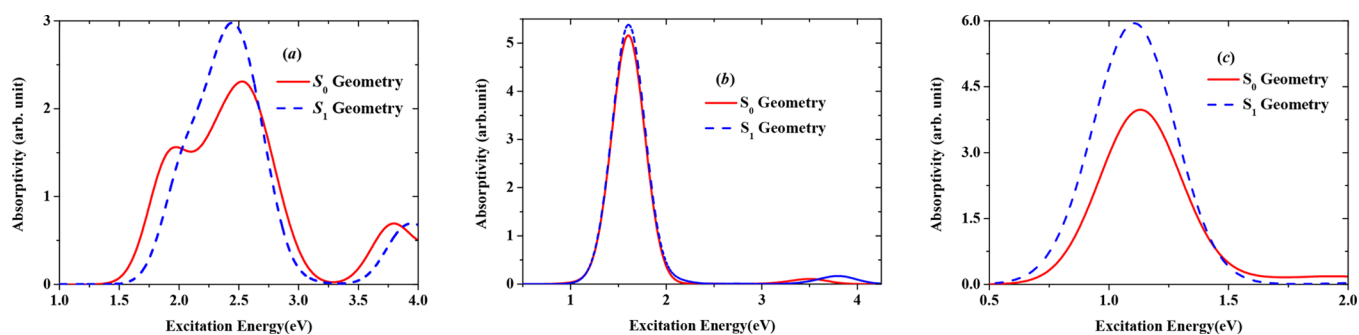


Figure 6. Simulated absorption spectra for ZnPc, DSB, and 3MT heptamer in the first singlet excited state in the S_0 and S_1 geometries. The hybrid functional of BHandHLYP was employed, and the spectra are obtained using the calculated oscillator strengths and the excitation energies broadened with the Gaussian function (FWHM = 0.4 eV). (a) ZnPc. (b) DSB. (c) 3MT heptamer.

C. Effect of Geometry Relaxation on ESA. To investigate the effect of geometry relaxation on ESA, we relax the structure with respect to the first singlet excited state, noted as S_1 . The ESA for ZnPc, DSB, and 3MT heptamer from the S_0 and S_1 geometries are compared in Figure 6. The effect of geometry relaxation on ESA is significant for ZnPc. The first two peaks (1.97 and 2.53 eV) in the spectrum for the S_0 geometry merge to one at 2.44 eV in the S_1 geometry. However, this effect is less pronounced for DSB, and the absorption peak is almost identical in the S_0 and S_1 geometries. For 3MT heptamer, even though the peak position is almost the same, the shape has changed from S_0 to S_1 .

Figure S2 in the Supporting Information displays the relaxed geometry for each system in the S_1 state. Geometrical difference for ZnPc and DSB in the S_0 and S_1 states is very small. This small geometry change results in noticeable changes of oscillator strength in ZnPc but not in DSB, which may be due to its open chain structure. Ling et al. reported a similar result that the lowest optically active ESA transitions of oligomers (F3–F7) in the S_0 and S_1 geometries almost coincide.¹² For 3MT heptamer, the geometrical differences in the S_0 and S_1 states are very large. As shown in Figure S2c, all the atoms of 3MT heptamer in the S_1 state are in the same plane, while that in the S_0 state is nonplanar, as reported by Roseli et al.⁹ This may explain the considerable increase of the absorption as the structure changes from the S_0 to the S_1 geometry. That the peak position in 3MT heptamer is not changed may also be attributed to the fact that the 3MT heptamer has a chain structure. In their study of fluorene polymer, Denis et al.²⁹ also found that ESA spectra are rather insensitive to geometric relaxation.

IV. DISCUSSION

Our paper shows that a single LR-TDDFT calculation can predict accurately the first singlet ESA spectra of ZnPc, DSB, and 3MT heptamer. While QR-TDDFT is rigorous in theory for ESA from the theoretical point of view, its implementation is much more complicated than current method based on LR-TDDFT. Nevertheless, the accuracy of the predicted data can be very close to that of QR-TDDFT. For example, in 3MT heptamer, the peak at 1.23 eV (see Table 3) is in excellent agreement with the QR-TDDFT result at 1.22 eV with the same functional CAM-B3LYP.⁹ For DSB, the peak position at 1.66 eV in Table 2 differs from that of QR-TDDFT by 0.15 eV. However, the QR-TDDFT result was calculated without considering the solvent effect.¹¹ Our data has the solvent effect included by the PCM method to compare with experimental measurement conducted in dioxane. In order to compare with the QR-TDDFT result, we recalculated the ESA in vacuum by using the 6-311G(d,p) basis set. Then, the peak shifts to 1.54 eV, which is in excellent agreement with the result of QR-TDDFT (1.51 eV).

It should be pointed out that the present LR-TDDFT method for ESA is different with the previous proposed LR-TDDFT methods (ATDA and SLR).^{25,27} In our algorithm, one only solves the equations of LR-TDDFT then constructs the wavefunctions for the excited states to calculate the oscillator strength. The wavefunctions are simply constructed from the LR-TDDFT formalism, which may be unusual with respect to those from the solutions of the Schrödinger equation. However, the formalism has been very successful for the study of excited-state dynamics.^{33,37–39} In the ATDA method, the transition moments between two excited states are estimated based on the coupled electronic oscillator (CEO) formalism, which is totally

different with the present method.²⁵ For the SLR method, one has to do the normal LR-TDDFT calculations two times, and the transition moments between two excited-states are obtained by comparing the transition dipoles from the two LR-TDDFT calculations.²⁷ Accordingly, the present formalism is much simpler than ATDA and SLR.

It is well-known that the TDDFT result depends on the functional model used. For the ground-state absorption spectra, there are quite a few empirical rules concerning the choice of a functional. The rules for ESA are still to be investigated. For the singlet ESA of ZnPc, the present study shows that BHandHLYP gives the best performance, as shown in Table 1. For the remaining two systems DSB and 3MT heptamer, BHandHLYP and CAM-B3LYP both give good agreement with the experimental measurements. For global hybrids functionals, the results recommend that a functional with a fraction of exact-exchange around 50% is preferred. Popular functionals for the ground state, B3LYP (20% HF) and M06 (27% HF), perform poorly compared to the experimental values in all three systems. The observations are consistent with the previous reports.^{8,11,9,56,57} For the singlet ESA of ZnPc, Fischer et al.'s RT-TDDFT calculations also favor BHandHLYP and CAM-B3LYP.⁸ For DSB and 3MT heptamer, CAM-B3LYP functional was recommended by Oliveira et al. and Roseli et al. for the singlet ESA based on QR-TDDFT results.^{9,11}

V. CONCLUSIONS

A method is proposed to calculate ESA spectra with a single LR-TDDFT calculation, the computational cost thus scale as N^4 . ESA spectra for the ZnPc, DSB, and 3MT heptamer are calculated with different exchange-correlation functionals. The hybrid functionals with a low percentage (<30%) of exact-exchange are not recommended. Among the functional models tested, BHandHLYP is outstanding as the best in all three systems, with the largest deviation from the experimental data around only 0.07 eV. The performance of long-range corrected functional CAM-B3LYP is also quite good, especially for DSB. It was pointed out by Bates and Furche that the functionals based on the meta-GGA (MGGA) may not be advisable for excited states as the gauge variance of the kinetic energy density with the MGGA.⁵⁸ The present results of the M06 (hybrid-meta-GGA) functional also advocate this observation. It is found that de-excitation causes a small red shift in the spectrum, and that the effect of geometry relaxation is system-dependent.

■ ASSOCIATED CONTENT

Supporting Information

The Supporting Information is available free of charge at <https://pubs.acs.org/doi/10.1021/acs.jpcc.9b10335>.

Positions of prominent features in the first singlet excited-state absorption spectrum of ZnPc predicted by the present method with various basis sets (Table S1), Cartesian coordinates of ZnPc, DSB, and 3MT-Heptamer in the S_0 state (Table S2), ESA spectra for ZnPc, DSB, and 3MT-Heptamer based on TDDFT and TDA/TDDFT with the CAM-B3LYP functional (Figure S1), and geometries in the S_0 and S_1 states (Figure S2) (PDF)

■ AUTHOR INFORMATION

Corresponding Authors

Xiaowei Sheng — Anhui Province Key Laboratory of Optoelectric Materials Science and Technology, Anhui Laboratory of

Molecule-Based Materials and The Key Laboratory of Functional Molecular Solids, Ministry of Education, Anhui Normal University, Anhui, Wuhu 241000, China; orcid.org/0000-0003-0311-7741; Email: xwsheng@mail.ahnu.edu.cn

Jian Wang — School of Science, Huzhou University, Zhejiang 10083, China; Email: jwang572@hotmail.com

Authors

Hongjuan Zhu — Anhui Province Key Laboratory of Optoelectric Materials Science and Technology, Anhui Laboratory of Molecule-Based Materials and The Key Laboratory of Functional Molecular Solids, Ministry of Education, Anhui Normal University, Anhui, Wuhu 241000, China

Kai Yin — Anhui Province Key Laboratory of Optoelectric Materials Science and Technology, Anhui Laboratory of Molecule-Based Materials and The Key Laboratory of Functional Molecular Solids, Ministry of Education, Anhui Normal University, Anhui, Wuhu 241000, China

Jichao Chen — Anhui Province Key Laboratory of Optoelectric Materials Science and Technology, Anhui Laboratory of Molecule-Based Materials and The Key Laboratory of Functional Molecular Solids, Ministry of Education, Anhui Normal University, Anhui, Wuhu 241000, China

Chunrui Wang — State Key Laboratory of Laser Interaction with Matter, Changchun Institute of Optics, Fine Mechanics and Physics, Chinese Academy of Science, Changchun 130033, China

Junfeng Shao — State Key Laboratory of Laser Interaction with Matter, Changchun Institute of Optics, Fine Mechanics and Physics, Chinese Academy of Science, Changchun 130033, China

Fei Chen — State Key Laboratory of Laser Interaction with Matter, Changchun Institute of Optics, Fine Mechanics and Physics, Chinese Academy of Science, Changchun 130033, China

Complete contact information is available at:

<https://pubs.acs.org/10.1021/acs.jpcc.9b10335>

Notes

The authors declare no competing financial interest.

■ ACKNOWLEDGMENTS

We thank Prof. E.J. Baerends and F. Wang for enlightening discussions. This work has been supported by the Jilin Province Science Fund for Excellent Young Scholar (no. 20180520189JH), Fund of the State Key Laboratory of Laser Interaction with Matter, China (SKLLIM1602), Key Research Program of Frontier Sciences, CAS (QYZDB-SSW-SLH014), Youth Innovation Promotion Association, CAS (2019220), The Key Laboratory of Functional Molecular Solids, Ministry of Education (FMS201933), and Anhui Laboratory of Molecule-Based Materials (no. fzj19010).

■ REFERENCES

- (1) Malinauskas, M.; Žukauskas, A.; Hasegawa, S.; Hayasaki, Y.; Mizeikis, V.; Buividas, R.; Juodkazis, S. Ultrafast Laser Processing of Materials: from Science to Industry. *Light: Sci. Appl.* **2016**, *5*, No. e16133.
- (2) Pascal, S.; Bellier, Q.; David, S.; Bouit, P.-A.; Chi, S.-H.; Makarov, N. S.; Guennic, B. L.; Chibani, S.; Berginc, G.; Feneyrou, P.; et al. Unraveling the Two-Photon and Excited-State Absorptions of Aza-BODIPY Dyes for Optical Power Limiting in the SWIR Band. *J. Phys. Chem. C* **2019**, *123*, 23661–23673.
- (3) Bhattacharya, S.; Biswas, C.; Raavi, S. S. K.; Krishna, J. V. S.; Krishna, N. V.; Giribab, L.; Soma, V. R. Synthesis, Optical, Electrochemical, DFT Studies, NLO Properties and Ultrafast Excited State

Dynamics of Carbazole-Induced Phthalocyanine Derivatives. *J. Phys. Chem. C* **2019**, *123*, 11118–11133.

(4) Liang, G.; Tao, L.; Tsang, Y. H.; Zeng, L.; Liu, X.; Li, J.; Qu, J.; Wen, Q. Optical Limiting Properties of a Few-Layer MoS₂/PMMA Composite under Excitation of Ultrafast Laser Pulses. *J. Mater. Chem. C* **2019**, *7*, 495–502.

(5) Chen, K.; Su, W.; Wang, Y.; Ge, H.; Zhang, K.; Wang, Y.; Xie, X.; Gomes, V. G.; Sun, H.; Huang, L. Nanocomposites of Carbon Nanotubes and Photon Upconversion Nanoparticles for Enhanced Optical Limiting Performance. *J. Mater. Chem. C* **2018**, *6*, 7311–7316.

(6) Perumbilavil, S.; López-Ortega, A.; Tiwari, G. K.; Nogués, J.; Endo, T.; Philip, R. Enhanced Ultrafast Nonlinear Optical Response in Ferrite Core/Shell Nanostructures with Excellent Optical Limiting Performance. *Small* **2018**, *14*, 1701001.

(7) Chen, S.; Fang, W.-H.; Zhang, L.; Zhang, J. Atomically Precise Multimetallic Semiconductive Nanoclusters with Optical Limiting Effects. *Angew. Chem., Int. Ed.* **2018**, *57*, 11252–11256.

(8) Fischer, S. A.; Cramer, C. J.; Govind, N. Excited-State Absorption from Real-Time Time-Dependent Density Functional Theory: Optical Limiting in Zinc Phthalocyanine. *J. Phys. Chem. Lett.* **2016**, *7*, 1387–1391.

(9) Roseli, R. B.; Tapping, P. C.; Kee, T. W. Origin of the Excited-State Absorption Spectrum of Polythiophene. *J. Phys. Chem. Lett.* **2017**, *8*, 2806–2811.

(10) Bai, Y.; Olivier, J. H.; Yoo, H.; Polizzi, N. F.; Park, J.; Rawson, J.; Therien, M. J. Molecular Road Map to Tuning Ground State Absorption and Excited State Dynamics of Long-Wavelength Absorbers. *J. Am. Chem. Soc.* **2017**, *139*, 16946–16958.

(11) Oliveira, E. F.; Shi, J.; Lavarda, F. C.; Lúer, L.; Milián-Medina, B.; Gierschner, J. Excited State Absorption Spectra of Dissolved and Aggregated Distyrylbenzene: A TD-DFT State and Vibronic Analysis. *J. Chem. Phys.* **2017**, *147*, No. 034903.

(12) Ling, S.; Schumacher, S.; Galbraith, I.; Paterson, M. J. Excited-State Absorption of Conjugated Polymers in the Near-Infrared and Visible: A Computational Study of Oligofluorenes. *J. Phys. Chem. C* **2013**, *117*, 6889–6895.

(13) Liu, B.-Q.; Wang, L.; Gao, D.-Y.; Zou, J.-H.; Ning, H.-L.; Peng, J.-B.; Cao, Y. Extremely high-efficiency and ultrasimplified hybrid white organic light-emitting diodes exploiting double multifunctional blue emitting layers. *Light: Sci. Appl.* **2016**, *5*, No. e16137.

(14) Savolainen, J.; van der Linden, D.; Dijkhuizen, N.; Herek, J. L. Characterizing the Functional Dynamics of Zinc Phthalocyanine from Femtoseconds to Nanoseconds. *J. Photochem. Photobiol., A* **2008**, *196*, 99–105.

(15) Theisen, R. F.; Huang, L.; Fleetham, T.; Adams, J. B.; Li, J. Ground and Excited States of Zinc Phthalocyanine, Zinc Tetrabenzoporphyrin, and Azaporphyrin Analogs Using DFT and TDDFT with Franck-Condon Analysis. *J. Chem. Phys.* **2015**, *142*, No. 094310.

(16) Adamo, C.; Jacquemin, D. The Calculations of Excited-State Properties with Time-Dependent Density Functional Theory. *Chem. Soc. Rev.* **2013**, *42*, 845–856.

(17) Yanagisawa, S.; Yasuda, T.; Inagaki, K.; Morikawa, Y.; Manseki, K.; Yanagida, S. Intermolecular Interaction as the Origin of Red Shifts in Absorption Spectra of Zinc-Phthalocyanine from First-Principles. *J. Photochem. Photobiol., A* **2013**, *117*, 11246–11253.

(18) Marom, N.; Hod, O.; Scuseria, G. E.; Kronik, L. Electronic Structure of Copper Phthalocyanine: A Comparative Density Functional Theory Study. *J. Chem. Phys.* **2008**, *128*, 164107.

(19) Liao, M. S.; Scheiner, S. Electronic Structure and Bonding in Metal Phthalocyanines, Metal = Fe, Co, Ni, Cu, Zn, Mg. *J. Chem. Phys.* **2001**, *114*, 9780–9791.

(20) Ricciardi, G.; Rosa, A.; Baerends, E. J. Ground and Excited States of Zinc Phthalocyanine Studied by Density Functional Methods. *J. Phys. Chem. A* **2001**, *105*, 5242–5254.

(21) Salek, P.; Vahtras, O.; Helgaker, T.; Ågren, H. Density-Functional Theory of Linear and Nonlinear Time-Dependent Molecular Properties. *J. Chem. Phys.* **2002**, *117*, 9630–9645.

(22) Cronstrand, P.; Christiansen, O.; Norman, P.; Ågren, H. Theoretical Calculations of Excited State Absorption. *J. Chem. Phys.* **2000**, *2*, 5357–5363.

(23) Hettema, H.; Jensen, H. J. A.; Joergensen, P.; Olsen, J. Quadratic response functions for a multiconfigurational self-consistent field wave function. *J. Chem. Phys.* **1992**, *97*, 1174–1190.

(24) Takimoto, Y.; Vila, F. D.; Rehr, J. J. Real-Time Time-Dependent Density Functional Theory Approach for Frequency-Dependent Nonlinear Optical Response in Photonic Molecules. *J. Chem. Phys.* **2007**, *127*, 154114.

(25) Mikhailov, I. A.; Tafur, S.; Masunov, A. E. Double excitations and state-to-state transition dipoles in $\pi - \pi^*$ excited singlet states of linear polyenes: Time-dependent density-functional theory versus multiconfigurational methods. *Phys. Rev. A* **2008**, *77*, No. 012510.

(26) Bowman, D. N.; Asher, J. C.; Fischer, S. A.; Cramer, C. J.; Govind, N. Excited-State Absorption in Tetrapyrrolyl Porphyrins: Comparing Real-Time and Quadratic-Response Time-Dependent Density Functional Theory. *Phys. Chem. Chem. Phys.* **2017**, *19*, 27452–27462.

(27) Mosquera, M. A.; Chen, L. X.; Ratner, M. A.; Schatz, G. C. Sequential Double Excitations from Linear-Response Time-Dependent Density Functional Theory. *J. Chem. Phys.* **2016**, *144*, 204105.

(28) Mosquera, M. A.; Jackson, N. E.; Fauvell, T. J.; Kelley, M. S.; Chen, L. X.; Schatz, G. C.; Ratner, M. A. Exciton Absorption Spectra by Linear Response Methods: Application to Conjugated Polymers. *J. Am. Chem. Soc.* **2017**, *139*, 3728–3735.

(29) Denis, J. C.; Ruseckas, A.; Hedley, G. J.; Matheson, A. B.; Paterson, M. J.; Turnbull, G. A.; Samuel, I. D. W.; Galbraith, I. Self-Trapping and Excited State Absorption in Fluorene Homo-Polymer and Copolymers with Benzothiadiazole and Tri-Phenylamine. *Phys. Chem. Chem. Phys.* **2016**, *18*, 21937–21948.

(30) Nayyar, I. H.; Masunov, A. E.; Tretiak, S. Comparison of TD-DFT Methods for the Calculation of Two-Photon Absorption Spectra of Oligophenylvinylenes. *J. Phys. Chem. C* **2013**, *117*, 18170–18189.

(31) Herbert, J. M.; Zhang, X.; Morrison, A. F.; Liu, J. Beyond Time-Dependent Density Functional Theory Using Only Single Excitations: Methods for Computational Studies of Excited States in Complex Systems. *Acc. Chem. Res.* **2016**, *49*, 931–941.

(32) Dreuw, A.; Head-Gordon, M. Single-Reference ab Initio Methods for the Calculation of Excited States of Large Molecules. *Chem. Rev.* **2005**, *105*, 4009–4037.

(33) Tapavicza, E.; Tavernelli, I.; Rothlisberger, U. Trajectory Surface Hopping within Linear Response Time-Dependent Density-Functional Theory. *Phys. Rev. Lett.* **2007**, *98*, No. 023001.

(34) Lu, T.; Chen, F. Multiwfn-A Multifunctional wavefunction analyzer-Software Manual, Version 3.7(dev). <http://sobereva.com/multiwfn/> (accessed Dec 22, 2019).

(35) Werner, U.; Mitrić, R.; Suzuki, T.; Bonačić-Koutecký, V. Nonadiabatic Dynamics within the Time Dependent Density Functional Theory: Ultrafast Photodynamics in Pyrazine. *Chem. Phys.* **2008**, *349*, 319–324.

(36) Casida, M. E. In *Recent Advances in Density Functional Methods*; World Scientific: Singapore, 1995.

(37) Tavernelli, I.; Tapavicza, E.; Rothlisberger, U. Nonadiabatic Coupling Vectors within Linear Response Time-Dependent Density Functional Theory. *J. Chem. Phys.* **2009**, *130*, 124107.

(38) Tavernelli, I.; Curchod, B. F. E.; Rothlisberger, U. On Nonadiabatic Coupling Vectors in Time-Dependent Density Functional Theory. *J. Chem. Phys.* **2009**, *131*, 196101.

(39) Tavernelli, I.; Curchod, B. F. E.; Laktionov, A.; Rothlisberger, U. Nonadiabatic Coupling Vectors for Excited States within Time-Dependent Density Functional Theory in the Tamm–Dancoff Approximation and Beyond. *J. Chem. Phys.* **2010**, *133*, 194104.

(40) Casida, M. E. Time-dependent density-functional theory for molecules and molecular solids. *J. Mol. Struct.: THEOCHEM* **2009**, *914*, 3–18.

(41) Becke, A. D. A New Mixing of Hartree-Fock and Local Density-Functional Theories. *J. Chem. Phys.* **1993**, *98*, 1372–1377.

- (42) Zhao, Y.; Truhlar, D. G. The M06 Suite of Density Functionals for Main Group Thermochemistry, Thermochemical Kinetics, Non-covalent Interactions, Excited States, and Transition Elements: Two New Functionals and Systematic Testing of Four M06-Class Functionals and 12 other Functionals. *Theor. Chem. Acc.* **2008**, *120*, 215–241.
- (43) Lee, C.; Yang, W.; Parr, R. G. Development of the Colle-Salvetti Correlation-Energy Formula into a Functional of the Electron Density. *Phys. Rev. B* **1988**, *37*, 785–789.
- (44) Yanai, T.; Tew, D. P.; Handy, N. C. A New Hybrid Exchange–Correlation Functional Using the Coulomb-Attenuating Method (CAM-B3LYP). *Chem. Phys. Lett.* **2004**, *393*, 51–57.
- (45) Chai, J.-D.; Head-Gordon, M. Long-Range Corrected Hybrid Density Functionals with Damped Atom-Atom Dispersion Corrections. *Phys. Chem. Chem. Phys.* **2008**, *10*, 6615–6620.
- (46) Lehtonen, O.; Sundholm, D.; Send, R.; Johansson, M. P. Coupled-Cluster and Density Functional Theory Studies of the Electronic Excitation Spectra of Trans-1,3-Butadiene and Trans-2-Propeniminium. *J. Chem. Phys.* **2009**, *131*, No. 024301.
- (47) Schmidt, M. W.; Baldridge, K. K.; Boatz, J. A.; Elbert, S. T.; Gordon, M. S.; Jensen, J. H.; Koseki, S.; Matsunaga, N.; Nguyen, K. A.; Su, S.; et al. General Atomic and Molecular Electronic Structure System. *J. Comput. Chem.* **1993**, *14*, 1347–1363.
- (48) Liang, K.; Zheng, C.; Wang, K.; Liu, W.; Guo, Z.; Li, Y.; Zhang, X. Theoretical Investigation of the Singlet-Triplet Splittings for Carbazole-Based Thermally Activated Delayed Fluorescence Emitters. *Phys. Chem. Chem. Phys.* **2016**, *18*, 26623–26629.
- (49) Goerigk, L.; Grimme, S. Assessment of TD-DFT Methods and of Various Spin Scaled CIS(D) and CC2 Versions for the Treatment of Low-Lying Valence Excitations of Large Organic Dyes. *J. Chem. Phys.* **2010**, *132*, 184103.
- (50) Ginocchietti, G.; Cecchetto, E.; De Cola, L.; Mazzucato, U.; Spalletti, A. Photobehaviour of Thio-Analogues of Stilbene and 1,4-Distyrylbenzene Studied by Time-Resolved Absorption Techniques. *Chem. Phys.* **2008**, *352*, 28–34.
- (51) Tapping, P. C.; Kee, T. W. Optical Pumping of Poly(3-hexylthiophene) Singlet Excitons Induces Charge Carrier Generation. *J. Phys. Chem. Lett.* **2014**, *5*, 1040–1047.
- (52) Kraabel, B.; Moses, D.; Heeger, A. J. Direct Observation of the Intersystem Crossing in Poly(3-Octylthiophene). *J. Chem. Phys.* **1995**, *103*, 5102–5108.
- (53) Fetter, A. L.; Walecka, J. D. *Quantum Theory of Many-Particle Systems*; McGraw-Hill: New York, 1971.
- (54) Hirata, S.; Head-Gordon, M. Time-Dependent Density Functional Theory within the Tamm–Dancoff Approximation. *Chem. Phys. Lett.* **1999**, *314*, 291–299.
- (55) Hutter, J. Excited State Nuclear Forces from the Tamm–Dancoff Approximation to Time-Dependent Density Functional Theory within the Plane Wave Basis Set Framework. *J. Chem. Phys.* **2003**, *118*, 3928–3934.
- (56) Laurent, A. D.; Jacquemin, D. TD-DFT Benchmarks: A Review. *Int. J. Quantum Chem.* **2013**, *113*, 2019–2039.
- (57) Wu, C.; Tretiak, S.; Chernyak, V. Y. Excited States and Optical Response of a Donor-Acceptor Substituted Polyene: A TD-DFT Study. *Chem. Phys. Lett.* **2007**, *433*, 305–311.
- (58) Bates, J. E.; Furche, F. Harnessing the Meta-Generalized Gradient Approximation for Time-Dependent Density Functional Theory. *J. Chem. Phys.* **2012**, *137*, 164105.